Gel Permeation Chromatography Characterization of the Chain Length Distributions in Thiol−Acrylate Photopolymer Networks

Amber E. Rydholm,[†] Nicole L. Held,[†] Christopher N. Bowman,[†,‡] and Kristi S. Anseth*[,†,§]

Chemical and Biological Engineering, University of Colorado, Boulder, Colorado 80309-0424; Restorative Dentistry, University of Colorado Health Sciences Center, Denver, Colorado 80045-0508; and Howard Hughes Medical Institute, University of Colorado, Boulder, Colorado 80309-0424

Received April 17, 2006; Revised Manuscript Received August 7, 2006

ABSTRACT: Cross-linked, degradable networks formed from the photopolymerization of thiol and acrylate monomers are explored as potential biomaterials. The degradation behavior and material properties of these networks are influenced by the molecular weight of the nondegradable thiol−polyacrylate backbone chains that form during photopolymerization. Here, gel permeation chromatography was used to characterize the thiol−polyacrylate backbone chain lengths in degraded thiol−acrylate networks. Increasing thiol functionality from 1 to 4 increased the backbone molecular weight ($\bar{M}_w = (2.3 \pm 0.07) \times 10^4$ Da for monothiol and $(3.6 \pm 0.1) \times 10^4$ Da for tetrathiol networks). Decreasing thiol functional group concentration from 30 to 10 mol % also increased the backbone lengths ($\bar{M}_w = (7.3 \pm 1.1) \times 10^4$ Da for the networks containing 10 mol % thiol groups as compared to $(3.6 \pm 0.1) \times 10^4$ Da for 30 mol % thiol). Finally, the backbone chain lengths were probed at various stages of degradation, and an increase in backbone molecular weight was observed as mass loss progressed from 10 to 70%.

Introduction

Highly cross-linked, photopolymer networks formed from multivinyl monomers are currently being investigated for a variety of applications including coatings, adhesives, photolithography, and biomaterials for medicine and dentistry. Many of the advantages that make photopolymers attractive for such a wide variety of applications directly result from either the photopolymerization reaction or the cross-linked network structures that are formed by many of these reactions. For example, photopolymerization occurs under ambient conditions, does not require the addition of any solvent, and affords spatial and temporal reaction control.[1,2] Additionally, the highly cross-linked network structure inherent to these materials is easily tailored through variations in monomer chemistry and functionality or the polymerization conditions present during network formation. This flexibility allows facile tailoring of materials with a desired solvent resistance, mechanical strength, or cross-linking density.[3] Further, photopolymers are attractive for many potential biomaterial applications because network formation is possible under physiological conditions in the presence of tissues, cells, proteins, and DNA.[4−22]

Many of the applications involving cross-linked photopolymer networks involve materials that are formed from the chain growth polymerization of multivinyl monomers. Recently, there has been an emerging interest in networks formed from the photoinitiated step growth reaction of thiol- and ene-functionalized monomers.[23,24] Additionally, thiol−ene photopolymerizations exhibit a reduced sensitivity to oxygen inhibition during polymerization, afford greater control of network structure and mechanical properties, polymerize with little or no added photoinitiator, and have been cured to depths in excess of 10 cm.[25−27] As a result, thiol−ene polymers represent a unique class of materials to explore for applications requiring enhanced material property control during degradation.

Degradation in covalently cross-linked polymer networks is influenced by the network chemistry, the cross-link chemistry, and the network structure. Using the network structure to control degradation behavior is particularly attractive due to its simplicity: adjusting the monomer molecular weight, functionality, or concentration are all readily feasible.[28−30] Understanding how both the initial and partially degraded network structure changes as a function of polymerization conditions would significantly improve our ability to control and manipulate the diffusivity, permeability, equilibrium water content, elasticity, and modulus[31] of the bulk material.

The initial structure of degradable thiol−ene networks is a direct result of the polymerization mechanism that occurs during formation. Thiol−ene photopolymerization involves the propagation of thiyl radicals through the carbon−carbon double bonds of the ene functional groups to form carbon-based radicals (step 1). These carbon-based radicals then abstract a hydrogen from a thiol functional group in a chain transfer reaction to regenerate a thiyl radical (step 2).[23,24,27,32] These steps occur sequentially throughout the polymerizing system until a cross-linked network forms. In some thiol−ene systems, such as thiol-acrylate based formulations, the ene functional group is capable of homopolymerizing to an appreciable extent when the carbon-based radicals propagate through other ene functional groups before undergoing chain transfer to a thiol (step 3).[23,27,32]

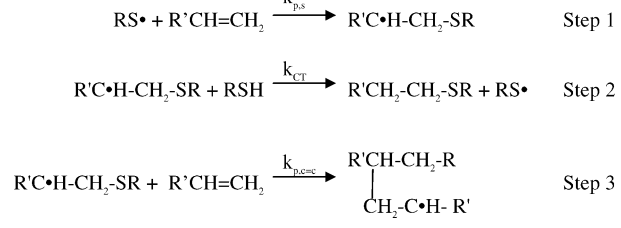

[†] Chemical and Biological Engineering, University of Colorado.
[‡] University of Colorado Health Sciences Center.
[§] Howard Hughes Medical Institute, University of Colorado.
* To whom correspondence should be addressed: Tel +1-303-492-3147; Fax +1-303-735-0095; e-mail kristi.anseth@colorado.edu.

10.1021/ma060858u CCC: $33.50
Published on Web 10/20/2006

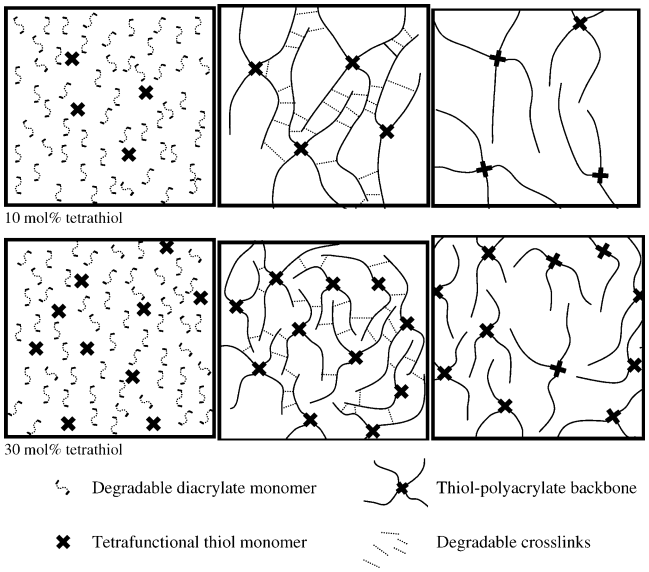

Figure 1. Depiction of the initial monomer mixture, polymerized network, and the backbone chains of the degraded network for thiol−acrylate photopolymers containing 10 and 30 mol % thiol functional groups. As polymer networks form from the two monomer solutions, the material synthesized from the solution with the higher thiol concentration has shorter thiol−polyacrylate backbone chains with fewer degradable cross-links connecting these chains to the network. This difference in thiol−polyacrylate chain length impacts the network's material properties and degradation behavior. Differences in thiol−polyacrylate chain length distributions were determined by isolating the thiol−polyacrylate chains and analyzing them with GPC.

Thiol−acrylate networks are influenced both by the monomer chemistry and by the structure of the network connections that form during polymerization. Variations in network structure caused during polymerization are the focus of this research and are influenced by three main parameters: (1) the probability that an acrylate group homopolymerizes relative to the probability that it undergoes chain transfer to thiol, (2) the initial ratio of thiol and acrylate functional groups, and (3) the thiol monomer functionality.

The acrylate homopolymerization probability is described by the ratio of the acrylate homopolymerization rate constant relative to the chain transfer rate constant ($k_{p,c=c}/k_{CT}$) and is measured experimentally by observing real-time changes in the thiol and acrylate FTIR peak areas during network formation.[23,27,33] This ratio of kinetic rate constants provides information about the amount of acrylate homopolymerization that occurs during network formation, which dictates the number of acrylates that react with each thiol. These thiol−acrylate oligomers then form the network's nondegradable thiol−polyacrylate backbone chains. The length of these backbone chains directly influences the network's degradation behavior and mechanical properties.[23,27,32] The $k_{p,c=c}/k_{CT}$ ratio changes depending on monomer chemistry but is independent of the ratio of thiol and acrylate functional groups.[33]

The initial ratio of thiol to acrylate functional groups also impacts the number of acrylate groups that homopolymerize from each reacted thiol group. This behavior is depicted schematically in Figure 1. Here, as the initial ratio of thiol to acrylate functional groups is increased, the length of the thiol−polyacrylate backbone chains decreases due to an increase in the number of chain transfer reactions that occur. The resulting network has fewer degradable cross-links connecting each thiol−polyacrylate backbone chain to the rest of the network than does a material formed from a monomer solution with a lower initial thiol-to-acrylate ratio.

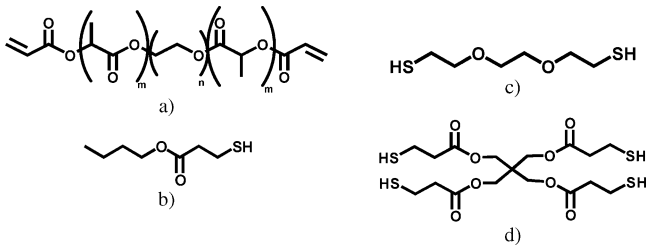

Figure 2. (a) $PEG_{2000}PLA_4$diacrylate ABA triblock monomer with a PEG core ($n = 45$), degradable poly(lactic acid) ($m = 3-4$), and photopolymerizable acrylate end groups, (b) butyl 3-mercaptopropionate (monothiol), (c) 2,2′-(ethylenedioxy)diethanethiol (dithiol), and (d) pentaerythritol tetrakis(3-mercaptopropionate) (tetrathiol).

The polymer network structure is also influenced by the thiol monomer functionality. If the thiol monomer functionality increases, the number of oligomeric acrylate chains attached to each thiol monomer also increases, effectively increasing the number of degradable cross-links connecting that thiol−polyacrylate backbone chain to the rest of the network.

While the influence of monomer functionality and functional group concentration on thiol−acrylate mass loss has been theoretically predicted and experimentally determined,[27,32] the network structures that are responsible for this observed behavior have only been briefly explored. The overall goal of this study was to utilize gel permeation chromatography (GPC) to investigate the chain length distributions of the thiol−polyacrylate backbone chains formed during the photopolymerization of various degradable thiol−acrylate systems. Samples were polymerized and degraded; the backbone chains were subsequently isolated from the rest of the degradation products, as depicted in Figure 1, and analyzed using GPC. First, the influence of the thiol monomer functionality and the thiol functional group concentrations on the backbone chain's distribution were each individually determined by isolating the thiol−polyacrylate backbone chains from the other degradation products. Next, the evolution of the distribution of backbone chain lengths during polymerization was investigated for various thiol-to-ene ratios by partially polymerizing the monomer mixtures to different conversions and analyzing the resulting networks' degradation products.

Finally, because network structure in degrading polymers is a dynamic property that influences many aspects of biomaterial performance, networks were polymerized and degraded in pH 7.4 phosphate buffer.[27] Samples were intermittently removed from the buffer and dried, creating a set of samples having varying mass loss percentages. Initially, as these networks degrade, the majority of their measured mass loss was due to the release of PEG from the core of the cross-links, and no significant change in the distribution of backbone chain lengths is expected. As mass loss continues and enough cross-links cleave, the shorter backbone chains should also start to release, shifting the chain length distribution toward a larger percentage of higher molecular weight chains.

Materials and Methods

Poly(lactic acid)-*b*-poly(ethylene glycol)-*b*-poly(lactic acid) Diacrylate. The degradable poly(lactic acid)-*b*-poly(ethylene glycol)-*b*-poly(lactic acid) diacrylated macromer (PEG2000PLA4diacrylate, Figure 2a) was prepared using techniques similar to those described by Sawhney et al.[34] and others.[27,29−32] The chemicals used to synthesize this monomer included poly(ethylene glycol) (PEG2000, $\bar{M}_n = 2000$ Da, Aldrich), stannous 2-ethylhexanoate (Sigma), DL-lactide (Polysciences), acryloyl chloride (Fluka), triethylamine (Fisher Scientific), and methylene chloride (Fisher Scientific). All reagents were used as received with the exception of methylene

chloride, which was dried with sodium sulfate (Fisher Scientific), vacuum-filtered, and stored over molecular sieves (Mallinckrodt). Analysis by ^{1}H NMR ($CDCl_3$): 1.55 ppm (33.86 H, PLA−O−CO−CH−CH_3−), 3.65 ppm (176.44 H, PEG−O−CH_2−CH_2−), 4.27 ppm (4.00 H, last H's on PEG next to PLA block), 5.17 ppm (10.42 H, PLA −O−CO−CH−CH_3−), 5.9 ppm (dd, 1.59 H, −COO−CH═CH_2), 6.17 ppm (q, 1.55 H, −COO−CH═CH_2), 6.47 ppm (dd, 1.61 H, −COO−CH═CH_2).

Thiol−Acrylate Monomer Mixture Preparation. Samples were prepared by mixing together the degradable acrylate monomer (Figure 2a) with various thiol monomers (0, 10, 30, and 50 mol % thiol functional groups) and 0.1 wt % 1-[4-(2-hydroxyethoxy)-phenyl]-2-hydroxy-2-methyl-1-propane-1-one (Irgacure 2959, I2959, Ciba) using a procedure previously described.[27] Monofunctional (butyl 3-mercaptopropionate, Figure 2b, Aldrich), difunctional (2,2′-(ethylenedioxy)diethanethiol, Figure 2c, Aldrich), and tetrafunctional (pentaerythritol tetrakis(3-mercaptopropionate), Figure 2d, Aldrich) thiol monomers were used.

Network Synthesis and Degradation. Disks were made from the various thiol−acrylate monomer mixtures using the following method: Equal weights of monomer mixture and dimethyl sulfoxide (DMSO, Fisher Scientific) were mixed in a disposable glass vial; the solution was pipetted into disk-shaped silicon rubber molds that were 10 mm in diameter and 0.9 mm thick and were sandwiched between two glass slides. The samples were exposed to 3.5 mW/cm^2 of 365 nm light for 10 min before being removed from the molds, placed into 0.6 mL microcentrifuge tubes, and degraded with 200 μL of 1 M NaOH (Fisher Scientific) for 10−30 min. Once the disks were fully degraded, 2 M HCl (Mallinckrodt) was added dropwise until the solution was neutralized and then slightly acidified. Under acidic conditions, the thiol−polyacrylate backbone chains precipitate from solution. All other degradation products remain in solution.

A portion of the disks were utilized in a mass loss study and were partially degraded in phosphate buffered saline solution for various amounts of time before being removed and dried as described elsewhere.[32] These partially degraded disks were then fully degraded, and their degradation products were analyzed using the methods described in the following section.

GPC Analysis of Backbone Chains. The thiol−polyacrylate precipitate was collected via centrifugation at 15 000 rpm for 10 min at 4 °C (Micromax RF, IEC). The thiol−polyacrylate pellets were then redissolved in 0.1 M phosphate buffer solution (pH of 7.4), and the thiol−polyacrylate chain lengths were characterized using gel permeation chromatography (GPC) (system: Waters 515 HPLC pump, 2410 refractive index detector; columns: Suprema 30A, 100A, 1000A, and Linear XL from Polymer Standards Service). These thiol−polyacrylate backbone chains are comprised of the polyacrylate chains and the multifunctional thiol monomers that form during photopolymerization. Their molecular weight depends on the number of thiol functional groups that are attached to a polyacrylate chain and the length of each of the attached polyacrylate chains. This distribution of thiol−polyacrylate backbone chain lengths is measured during GPC experiments.

The molecular weight values (x-axis of the graphs plotting GPC data) were estimated from poly(methacrylic acid) (PMAA) standards (poly(methacrylic acid) sodium salt, M_p = 1000−1 000 000, Polymer Standards Service, where M_p is the molecular weight at the peak maximum). The numbers resulting from this calibration are useful for observing trends in molecular weight but do not represent the exact molecular weights for these samples.

Deconvolution of GPC Chromatograms. Pure acrylate networks and thiol−acrylate networks formed from 10 mol % thiol monomer mixtures produced bimodal GPC chromatograms. These data were resolved into two peaks using PeakFit (Systat Software Inc., version 4.0). The following settings were used in the deconvolution procedure: the data were smoothed using the Savitzky−Golay algorithm, level 8.0; the data were deconvoluted using the Autofit Peaks III deconvolution macro using the chromatography and EMG settings.

Determining Partial-Cure Conversion Using Near-IR Characterization. To determine the acrylate conversions of partially cured samples, FTIR studies were completed using a Nicolet 750 Magna FTIR spectrometer with a KBr beam splitter, an MCT/A detector, and a white light IR source. Samples were prepared by placing thiol and acrylate monomer solutions between two glass microscope slides that were separated by a 0.9 mm thick piece of silicon rubber. These samples were placed in a horizontal transmission apparatus[35] that allowed in-situ observations of polymerization behavior during irradiation using series scans that obtained spectra at a rate of 1.08 scans/s. Samples were irradiated with 12 mW/cm^2 of 320−500 nm light (peak light intensity at 365 nm) using a Novacure light source (EXFO). Conversions were calculated using the ratio of the acrylate peak's area at 6165 cm^{-1} as a function of time to the initial peak area prior to irradiation.

Mid-IR Polymerization Characterization. To observe real-time polymerization kinetics, FTIR studies of thin-film samples were completed as described elsewhere.[27] Acrylate conversion was monitored using both the carbon−carbon double bond absorption double peak at 1636 and 1620 cm^{-1} and the out-of-plane stretch at 810 cm^{-1}. The thiol conversion was observed by measuring the area of the S−H absorption peak at 2560 cm^{-1}. Conversions were calculated using the ratio of the peak area as a function of time to the initial peak area prior to irradiation. Acrylate and thiol concentrations were calculated from the initial functional group concentrations and the measured conversion values.

Modeling the Distribution of Backbone Chains in Thiol−Acrylate Photopolymers. A theoretical model that predicts the distribution of thiol−polyacrylate backbone chains and bulk degradation behavior for these thiol−acrylate hydrogels is described in detail elsewhere.[32,36] This approach uses the initial thiol and acrylate functional group concentrations and the relative rates of the acrylate homopolymerization and chain transfer reactions to predict the number of acrylates that react with each thiol functional group at each extent of conversion. Briefly, the model first calculates the probability that an acrylic radical homopolymerizes (p_h, eq 1), relative to all possible propagation reactions. This parameter is then used to determine the probability of forming a thiol−polyacrylate chain of length n ($p(n)$, eq 2), which effectively yields the distribution of polyacrylate chain lengths at a given conversion. The summation of this distribution from zero conversion to the conversion of interest produces the overall distribution of polyacrylate chain lengths attached to each thiol group. For multifunctional thiol monomers the distribution of the number of acrylate groups attached is determined by statistically averaging the distribution of the polyacrylate chains on each arm of the thiol monomer. This last step assumes equal reactivity of each thiol group regardless of whether or not other thiol groups on the same monomer are reacted.[36] In eqs 1 and 2, p_h is the probability that an acrylate radical homopolymerizes, $k_{p,c=c}$ is the kinetic rate constant for acrylate homopolymerization, [C═C] is the concentration of acrylate functional groups, k_{CT} is the kinetic rate constant for the chain transfer reaction, [SH] is the concentration of thiol functional groups, and $p(n)$ is the probability that a polyacrylate chain containing n acrylate groups is formed.

$$p_h = \frac{k_{p,c=c}[C{=}C]}{k_{p,c=c}[C{=}C] + k_{CT}[SH]} \quad (1)$$

$$p(n) = p_h^{\,n-1}(1 - p_h) \quad (2)$$

Results and Discussion

Degradable networks were formed from the photopolymerization of multifunctional thiol and degradable acrylate monomers. Previous studies have focused on how variations in thiol monomer functionality and thiol functional group concentration impact experimental and theoretical mass loss behavior.[32,36] The work presented here aims to explore experimentally how changes in the initial monomer formulation impact the network

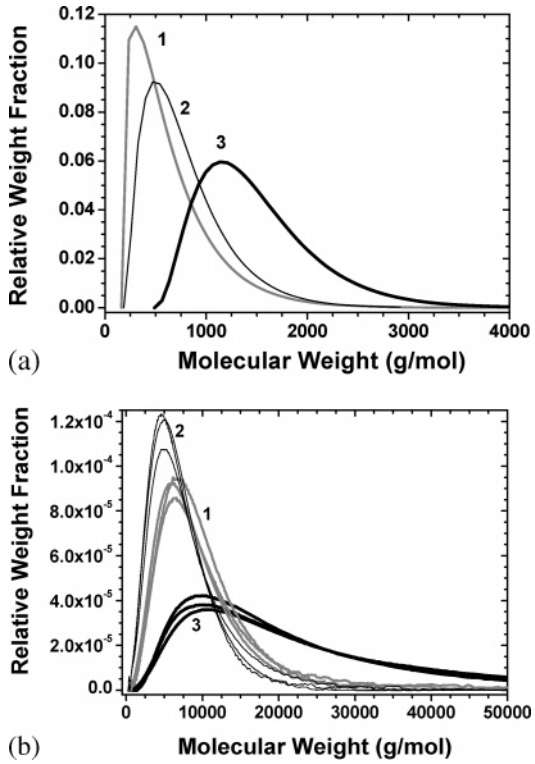

Figure 3. Model predictions (a) and GPC data (b) for thiol−acrylate photopolymers made from monomer mixtures containing 30 mol % thiol functional groups that originated from (1) mono-, (2) di-, and (3) tetrafunctional thiol monomers. The GPC data in (b) contain multiple repeats for each experimental condition. w_i is the weight fraction of backbone chains that have a particular molecular weight, and the area under each curve is normalized to 1.

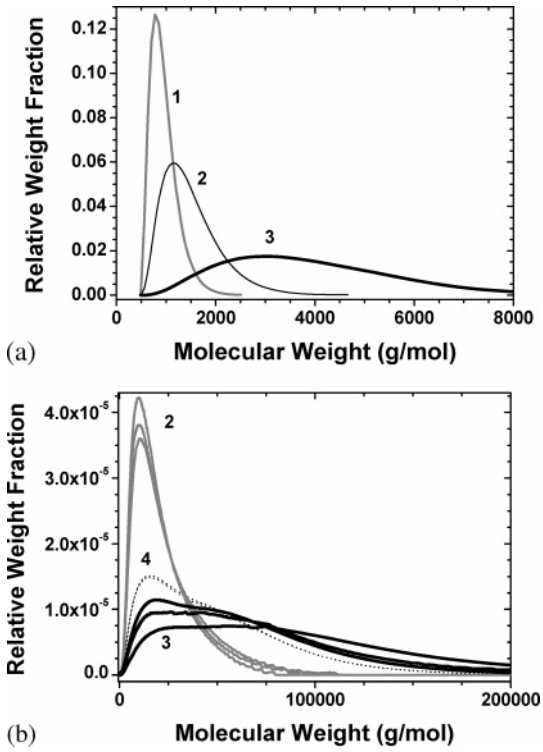

Figure 4. Model predictions (a) and GPC data for the degraded thiol−acrylate disks (b) for thiol−acrylate photopolymers made from monomer mixtures containing 50 mol % (1), 30 mol % (2), and 10 mol % (3) thiol functional groups that originated from tetrafunctional thiol monomers. In (b), a pure acrylate sample containing 0 mol % thiol functional groups (4) is also included for comparison. The GPC data in (b) contain multiple repeats for each experimental condition. w_i is the weight fraction of backbone chains that have a particular molecular weight, and the area under each curve is normalized to 1.

structure at the molecular level through GPC analysis of the degradation products, specifically the thiol−polyacrylate backbone chains. In addition, the evolution of the chain length distribution was studied both for samples that had been partially polymerized to various extents of conversion and for samples that had been partially degraded to various mass loss extents.

Impact of Thiol Functionality on the Distribution of Thiol−Polyacrylate Chains. Figure 3a shows the model predictions of how the distribution of backbone chains in thiol−acrylate photopolymers changes as a function of thiol monomer functionality. In this figure the weight fraction of the backbone chains of length i (w_i) is plotted as a function of the molecular weight that corresponds to a chain of length i. The backbone chain length distribution in polymer networks made from monomer solutions containing 70 mol % acrylate functional groups and 30 mol % thiol functional groups increased in both molecular weight and polydispersity (PDI) as the functionality of the thiol monomer was increased from 1 to 2 to 4. This increase in the molecular weight and the PDI of the backbone chains with increasing monomer functionality makes sense since the multifunctional thiol monomers effectively join multiple polyacrylate chains together. As the monomer functionality is increased, more polyacrylate chains are connected to each other in the backbone chains, increasing the molecular weight of the thiol−polyacrylate backbone chains.

Figure 3b displays the GPC data for the distribution of backbone chain lengths from degraded thiol−acrylate networks made from 70 mol % acrylate and 30 mol % thiol functional groups. Here, the tetrathiol's chain length distribution had the highest molecular weight averages ($\bar{M}_n = (2.6 \pm 0.08) \times 10^4$ Da and $\bar{M}_w = (3.6 \pm 0.1) \times 10^4$ Da), which was expected on the basis of model predictions of Figure 3a. The trend observed for the monothiol and dithiol GPC data, however, was reversed from what was predicted by the model. For the GPC data, the dithiol chain length distribution had the narrowest PDI and the lowest molecular weights ($\bar{M}_n = (9.4 \pm 0.9) \times 10^3$ Da and $\bar{M}_w = (1.7 \pm 0.03) \times 10^4$ Da vs $(1.6 \pm 0.1) \times 10^4$ Da and $(2.3 \pm 0.07) \times 10^4$ Da for the monothiol data).

Closer inspection of the monomer chemistry (Figure 2) and the polymerization kinetics[32] reveals that the shift in distribution of backbone chain lengths for the dithiol networks to lower $\bar{M}_n$ and $\bar{M}_w$ is most likely due to the dithiol monomer undergoing more chain transfer than the mono- or tetrathiol monomers, thereby reducing the amount of homopolymerization that occurs relative to chain transfer. At a given conversion and initial concentration of thiol and acrylate functional groups, an increase in homopolymerization leads to longer backbone chains whose population is more polydisperse, directly impacting the network structure in these cross-linked polymeric materials. Higher molecular weight backbone chains decrease the mass loss rate and the onset of reverse gelation for degrading thiol−acrylate networks.[32] Additionally, an increase in polydispersity corresponds to an increase in network heterogeneity, which often leads to a broadening of many thermomechanical properties.

Impact of Thiol Concentration on the Distribution of Thiol−Polyacrylate Chains. Figure 4 presents the model predictions and GPC data for thiol−acrylate networks made with varying ratios of thiol and acrylate functional groups. The model predictions in Figure 4a exhibit a decrease in PDI and a shift toward lower molecular weight chains when more thiol groups are present. This behavior is attributed to an increase in chain transfer that occurs during network formation with increasing

thiol concentration. Increasing the chain transfer rate decreases the amount of acrylate homopolymerization that occurs, shifting the backbone chain length distribution toward shorter chains. The reduction in PDI with increasing thiol functional groups follows similar logic. The more thiol groups that are available for chain transfer, the greater the number of polyacrylate chains that will undergo chain transfer after only a few homopolymerization reactions, reducing the PDI.

The normalized GPC data for the backbone chain length distribution in networks made from 0, 10, and 30 mol % thiol functional groups are shown in Figure 4b. No precipitate formed for the networks synthesized with 50 mol % tetrathiol, so no samples were obtained for GPC characterization. Oligomeric thiol−acrylate chains formed under these conditions were of sufficiently low molecular weight that they remained soluble. Alternative methods for collecting and isolating the backbone chains in these networks were not successful.

The relationship observed in Figure 4 between the distribution of thiol−polyacrylate chain lengths for networks synthesized from 30 and 10 mol % thiol functional groups exhibits the expected behavior based on the model results. The molecular weight averages for the backbone chains from these networks are $\bar{M}_n = (2.6 \pm 0.08) \times 10^4$ Da and $\bar{M}_w = (3.6 \pm 0.1) \times 10^4$ Da for the 30 mol % thiol networks and $\bar{M}_n = (3.1 \pm 0.5) \times 10^4$ Da and $\bar{M}_w = (7.3 \pm 1.1) \times 10^4$ Da for the 10 mol % networks. The appearance of bimodal peaks in the chain length distributions of the 10 and 0 mol % thiol samples, however, was not expected, particularly the appearance of a low molecular weight shoulder. While similar results have been observed for pure acrylate networks,[2,37] the mechanism responsible is not well understood.

In an attempt to understand further the formation of this bimodal distribution, experiments investigating whether or not the distribution changes during network formation were performed. Figure 5a exhibits bimodal GPC data obtained for the backbone chain length distribution of thiol−acrylate networks made from monomer solutions containing 10 mol % thiol functional groups that were cured to 10, 30, 40, 75, and 100% acrylate conversion. The data in Figure 5a shift toward lower molecular weights as the acrylate conversion increases. This apparent shift was confirmed by deconvoluting each of these bimodal peaks into two separate peaks. An example of the deconvolution is graphically represented in Figure 5b.

By deconvoluting the original GPC data, the shift in the backbone chain length distribution toward lower molecular weight chains was able to be quantified. The higher molecular weight fraction was calculated for all of the original peaks shown in Figure 5a and is plotted as a function of acrylate conversion in Figure 6. Examining these data reveals that the bimodal molecular weight distribution is initially dominated by high molecular weight chains. As conversion increases, the fraction of the molecular weight distribution being contributed by lower molecular weight chains increases until the lower molecular weight chains slightly dominate the distribution near 100% acrylate conversion.

The shift observed in Figure 6 toward lower molecular weight chains with increasing acrylate conversion might be due to a relative enriching of the polymerizing system with unreacted thiol groups. Figure 7 contains real-time mid-FTIR data for a polymerizing thiol−acrylate material initially containing 10 mol % thiol functional groups. For these samples, the initial ratio of acrylate to thiol groups is 9. When the sample is exposed to UV light, the thiol and acrylate groups react at different rates, changing the relative amounts of acrylate and thiol functional

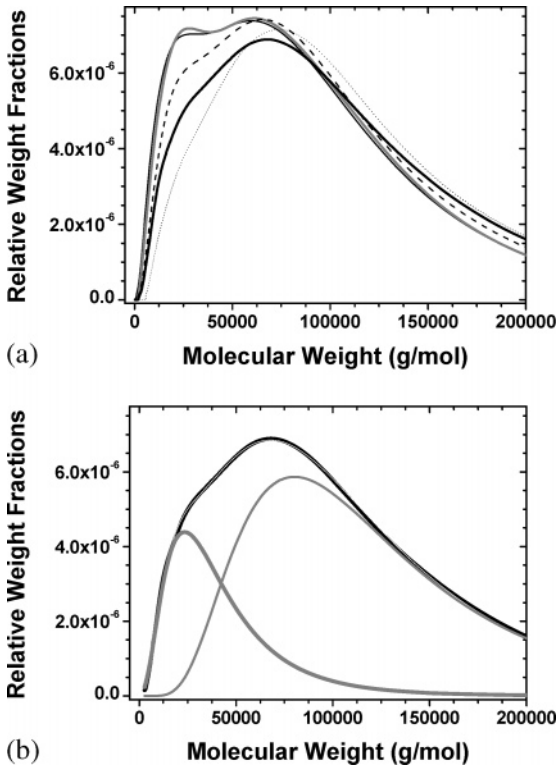

Figure 5. (a) GPC data for partially cured thiol−acrylate networks made from monomer mixtures initially containing 10 mol % tetrathiol functional groups. For each sample, acrylate conversion is 10% (···), 30% (bold —), 40% (- - -), 75% (gray —), and 100% (—). (b) Deconvolution of bimodal thiol−polyacrylate chromatogram from the network at 30% conversion. The original GPC chromatogram (bold —) was resolved into two underlying peaks of lower (gray —) and higher (gray —) molecular weight backbone chains. The sum of the two resolved peaks is shown in white, which overlays the black curve of the original data nearly perfectly. w_i is the weight fraction of backbone chains that have a particular molecular weight.

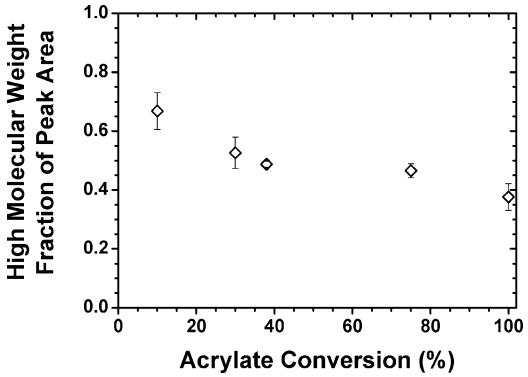

Figure 6. Fraction of the total backbone chain length distribution peak area in 10 mol % tetrathiol networks that is contributed by the higher molecular weight chains as a function of acrylate conversion.

groups. For this particular system the ratio of acrylate to thiol groups decreases with increasing acrylate conversion, corresponding to an increase in the number of thiol groups for every remaining acrylate group. This increase in the relative concentration of thiol groups results in an increase in the amount of chain transfer that occurs and reduces the molecular weight of the backbone chains being produced.

Changes in the Distribution of Backbone Chain Lengths with Network Degradation. Networks were synthesized from a tetrafunctional thiol−diacrylate mixture that initially contained 30 mol % thiol functional groups. These samples were then placed into degradation buffer for varying amounts of time, after

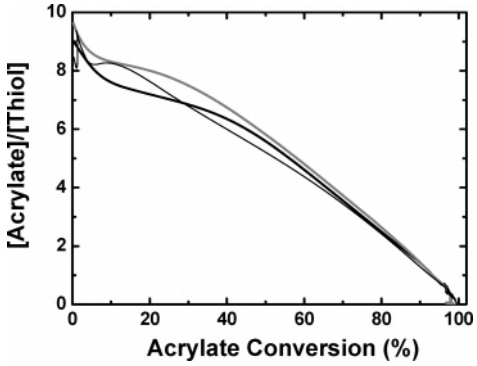

Figure 7. Ratio of acrylate and thiol functional group concentrations as a function of acrylate conversion for three repeats of the polymerization of thiol−acrylate networks made from 10 mol % tetrathiol monomer. Observe how the system becomes thiol-enriched as the polymerization proceeds.

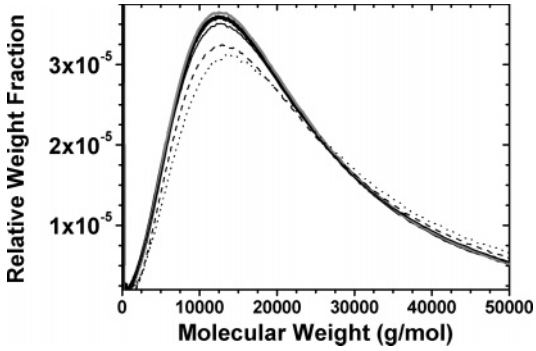

Figure 8. Changes in the backbone chain length distribution for a 30 mol % tetrathiol sample as a function of degradation time. The lines in (a) are representative distributions of the residual thiol−polyacrylate backbone chains after 5% (bold —), 10% (gray —), 35% (—), 60% (- - -), and 70% (•••) mass loss. The $\bar{M}_n$ and $\bar{M}_w$ of the thiol−polyacrylate chains from the samples exhibiting 60 and 70% mass loss are statistically different than the $\bar{M}_n$ and $\bar{M}_w$ of samples exhibiting less than 40% mass loss at the 99% confidence interval.

which they were removed and their mass loss was determined.[32] Figure 8 presents the GPC data obtained for the backbone chains that were isolated from partially degraded thiol−acrylate networks. Examining these data shows that as the extent of degradation increases, the chain length distribution initially remains unchanged. As the extent of mass loss exceeds 60%, however, the chain length distribution shifts toward higher molecular weight backbone chains. During these mass loss experiments, initial mass loss occurs as PEG is released from the core of each cross-link. The backbone chains are released primarily at later stages of degradation. Shorter backbone chains have fewer cross-links that must degrade before these chains are released. A model that was developed to predict mass loss in these types of thiol−acrylate networks[32] accounts for this shift in the distribution of backbone chain lengths throughout degradation, allowing experimental mass loss profiles to be accurately modeled.

In summary, the information provided by the data in this paper is extremely useful in understanding the network structure in these thiol−acrylate polymers. The thiol−acrylate networks are comprised of thiol−polyacrylate backbone chains and PEG-based degradable cross-links. The length of each polyacrylate chain is directly correlated to the number of cross-links that connect it to the rest of the network. Collectively looking at the distributions of thiol−polyacrylate backbone chains in Figures 3 and 4 provides insight concerning the structure of the entire thiol−acrylate network. Additionally, the data in Figures 5−8 provide valuable insight concerning the network formation mechanism that occurs during thiol−acrylate photopolymerization. While the topic of network structure in thiol−acrylate polymers has been the focus of previous work, the data in this paper further support and expand upon the findings originally presented by Cramer et al.[23]

Conclusions

GPC was used to characterize the thiol−polyacrylate degradation products from thiol−acrylate photopolymeric networks. This work confirms previous hypotheses that increases in thiol monomer functionality and decreases in thiol functional group concentration increase the average molecular weight and polydispersity of the distribution of thiol−polyacrylate backbone chains. Additionally, a bimodal chain length distribution was observed for networks made from 10 mol % tetrathiol. This distribution shifts toward shorter backbone chains as the extent of acrylate polymerization increases. Finally, a shift in the chain length distribution toward higher molecular weight chains was observed in degrading networks when the percent mass loss progressed from 10 to 70%. This is expected since shorter backbone chains have fewer cross-links and are released from the network at earlier stages of degradation.

While previous studies have demonstrated that thiol functional group concentration and thiol monomer functionality both impact mass loss profiles in degradable thiol−acrylate polymers, this work connects how these variations in monomer formulation impact the network structure of the polymer that is ultimately formed. Understanding the relationships between monomer formulation, network structure, and degradation behavior is a key component in the design of better materials for applications that require control and manipulation of degradation-dependent properties (e.g., biomaterials).

Acknowledgment. The authors thank their funding sources for this work, a grant from the NIH (R01 DE12998), a Department of Education Graduate Assistanceship in Areas of National Need (GAANN) fellowship and a University of Colorado Beverly Sears Graduate Student Grant to A.E.R., and a fellowship from the Undergraduate Research Opportunities Program at the University of Colorado to N.L.H.

References and Notes

(1) Lovestead, T. M.; Burdick, J. A.; Anseth, K. S.; Bowman, C. N. *Polymer* **2005**, *46*, 6226−6234.
(2) Burkoth, A. K.; Anseth, K. S. *Macromolecules* **1999**, *32*, 1438−1444.
(3) Burdick, J. A.; Lovestead, T. M.; Anseth, K. S. *Biomacromolecules* **2003**, *4*, 149−156.
(4) Burdick, J. A.; Anseth, K. S. *Biomaterials* **2002**, *23*, 4315−4323.
(5) Burdick, J. A.; Chung, C.; Jia, X. Q.; Randolph, M. A.; Langer, R. *Biomacromolecules* **2005**, *6*, 386−391.
(6) Burdick, J. A.; Mason, M. N.; Anseth, K. S. *J. Biomater. Sci., Polym. Ed.* **2001**, *12*, 1253−1265.
(7) Burdick, J. A.; Mason, M. N.; Hinman, A. D.; Thorne, K.; Anseth, K. S. *J. Controlled Release* **2002**, *83*, 53−63.
(8) Burdick, J. A.; Padera, R. F.; Huang, J. V.; Anseth, K. S. *J. Biomed. Mater. Res.* **2002**, *63*, 484−491.
(9) Burdick, J. A.; Peterson, A. J.; Anseth, K. S. *Biomaterials* **2001**, *22*, 1779−1786.
(10) Burdick, J. A.; Ward, M.; Liang, E.; Young, M.; Langer, R. *J. Neurotrauma* **2004**, *21*, 1311−1311.
(11) Poshusta, A. K.; Burdick, J. A.; Mortisen, D. J.; Padera, R. F.; Ruehlman, D.; Yaszemski, M. J.; Anseth, K. S. *J. Biomed. Mater. Res., Part A* **2003**, *64A*, 62−69.
(12) Behravesh, E.; Mikos, A. G. *J. Biomed. Mater. Res., Part A* **2003**, *66A*, 698−706.
(13) Behravesh, E.; Zygourakis, K.; Mikos, A. G. *J. Biomed. Mater. Res.* **2003**, *65A*, 260−270.
(14) Elbert, D. L.; Hubbell, J. A. *Biomacromolecules* **2001**, *2*, 430−441.

(15) Hern, D. L.; Hubbell, J. A. *J. Biomed. Mater. Res.* **1998**, *39*, 266−276.
(16) Lutolf, M. P.; Hubbell, J. A. *Biomacromolecules* **2003**, *4*, 713−722.
(17) Masters, K. S.; Shah, D. N.; Walker, G.; Leinwand, L. A.; Anseth, K. S. *J. Biomed. Mater. Res., Part A* **2004**, *71A*, 172−180.
(18) Nuttelman, C. R.; Tripodi, M. C.; Anseth, K. S. *Matrix Biol.* **2005**, *24*, 208−218.
(19) Masters, K. S.; Shah, D. N.; Leinwand, L. A.; Anseth, K. S. *Biomaterials* **2005**, *26*, 2517−2525.
(20) Quick, D. J.; Anseth, K. S. *Pharm. Res.* **2003**, *20*, 1730−1737.
(21) Quick, D. J.; Macdonald, K. K.; Anseth, K. S. *J. Controlled Release* **2004**, *97*, 333−343.
(22) Williams, C.; Malik, A.; Kim, T.; Manson, P.; Elisseeff, J. *Biomaterials* **2005**, *26*, 1211−1218.
(23) Cramer, N. B.; Bowman, C. N. *J. Polym. Sci., Part A: Polym. Chem.* **2001**, *39*, 3311−3319.
(24) Lecamp, L.; Houllier, B.; Youssef, B.; Bunel, C. *Polymer* **2001**, *42*, 2727−2736.
(25) Cramer, N. B.; Reddy, S. K.; Cole, M.; Hoyle, C. E.; Bowman, C. N. *J. Polym. Sci., Part A: Polym. Chem.* **2004**, *42*, 5817−5826.
(26) Cramer, N. B.; Scott, J. P.; Bowman, C. N. *Macromolecules* **2002**, *35*, 5361−5365.
(27) Rydholm, A. E.; Bowman, C. N.; Anseth, K. S. *Biomaterials* **2005**, *26*, 4495−4506.
(28) Martens, P. J.; Metters, A. T.; Anseth, K. S.; Bowman, C. N. *J. Phys. Chem. B* **2001**, *105*, 5131−5138.
(29) Metters, A. T.; Anseth, K. S.; Bowman, C. N. *J. Phys. Chem. B* **2001**, *105*, 8069−8076.
(30) Metters, A. T.; Anseth, K. S.; Bowman, C. N. *J. Phys. Chem. B* **2000**, *104*, 7043−7049.
(31) Martens, P. J.; Bryant, S. J.; Anseth, K. S. *Biomacromolecules* **2003**, *4*, 283−292.
(32) Rydholm, A. E.; Reddy, S. K.; Anseth, K. S.; Bowman, C. N. *Biomacromolecules*, in press.
(33) Cramer, N. B.; Reddy, S. K.; O'Brien, A. K.; Bowman, C. N. *Macromolecules* **2003**, *36*, 7964−7969.
(34) Sawhney, A. S.; Pathak, C. P.; Hubbell, J. A. *Macromolecules* **1993**, *26*, 581−587.
(35) Berchtold, K. A.; Bowman, C. N. In RadTech Europe 99 Conference Proceedings, Berlin, Germany, 1999; p 767.
(36) Reddy, S. K.; Anseth, K. S.; Bowman, C. N. *Polymer* **2005**, *46*, 4212−4222.
(37) Metters, A. T. Investigation of Degradable Crosslinked Hydrogels: Prediction of Degradation Behavior. Ph.D., University of Colorado, Boulder, CO, 2000.

MA060858U